Electron-phonon superconductivity in the filled skutterudites $LaRu_4P_{12}$, $LaRu_4As_{12}$, and $LaPt_4Ge_{12}$

H. M. Tütüncü,[1,2] Ertuğrul Karaca,[1] and G. P. Srivastava[3]

[1]*Sakarya Üniversitesi, Fen-Edebiyat Fakültesi, Fizik Bölümü, 54187 Adapazarı, Turkey*

[2]*Sakarya Üniversitesi, BIMAYAM Biyomedikal, Manyetik ve Yarıletken Malzemeler Araştırma Merkezi, 54187 Adapazarı, Turkey*

[3]*School of Physics, University of Exeter, Stocker Road, Exeter EX4 4QL, United Kingdom*

(Received 14 March 2017; revised manuscript received 10 June 2017; published 29 June 2017)

We have reported on the structural, elastic, electronic, lattice dynamical and electron-phonon interaction properties of LaT_4X_{12} (T = Ru, Pt and X = P, As, Ge) by using the generalized gradient approximation of the density functional theory and the plane-wave pseudopotential method. These lanthanum-filled skutterudites are found to be characterized with a flat band, resulting in a sharp peak in the electronic density of states, near the Fermi level. The lattice dynamical properties of these materials change considerably when the P atom is replaced by larger As or Ge atoms. The Migdal-Eliashberg approach is used to determine the Eliashberg spectral function for all the considered compounds. Using the calculated Eliashberg spectral function, the value of average electron-phonon coupling parameter is found to be 0.74 for $LaRu_4P_{12}$, 1.03 for $LaRu_4As_{12}$, and 1.08 for $LaPt_4Ge_{12}$. The superconducting critical temperature (T_c) values for $LaRu_4P_{12}$, $LaRu_4As_{12}$, and $LaPt_4Ge_{12}$ are estimated to be 6.95, 11.56, and 8.32 K, respectively, which compare well enough with their experimentally measured values of 7.2, 10.45, and 8.23 K.

DOI: 10.1103/PhysRevB.95.214514

I. INTRODUCTION

Filled skutterudite pnictides with the general formula LnT_4X_{12} (Ln = lanthanide, T = transition metal, X = pnictogen) have received considerable attention in recent years because of their interesting physical properties at low temperature, such as excellent thermoelectric performance [1–4], intermediate-valence [5], non-Fermi-liquid behavior [6], magnetic ordering [7–9], metal-to-insulator transition [10–16], semiconducting behavior [17–23], and heavy-fermion behavior [24–36]. Also, lanthanum compounds display interesting superconducting behavior at low temperatures [37–47]. The superconducting transition temperature (T_c) of $LaRu_4X_{12}$ with X = P, As, Sb is found to be 7.2, 10.3, and 2.8 K [37,38,42,43].

Recently, superconducting properties of the filled skutterudite compound $LaRu_4As_{12}$ have been investigated as a function of both temperature and magnetic field in the experimental work of Bochenek and co-workers [46]. These authors took advantage of its high critical temperature (T_c) and high critical field ($H_{c2} \sim 10.2$ T) to make investigations in a wide range of temperatures and magnetic fields. They observed a nonlinear magnetic field dependence of the specific heat in the limit $T \to 0$ K, a positive curvature of the upper critical field in the vicinity of T_c, and a deviation of the electronic specific heat from the one-gap α model. These behaviors were interpreted, in contrast to other skutterudites, as evidence that $LaRu_4As_{12}$ is an example of a multiband s-wave superconductor.

In 2007, Bauer and co-workers [48] managed to synthesize new germanium-platinum compounds MPt_4Ge_{12} (M = Sr, Ba) with the filled-skutterudite crystal structure and observed the superconductivity with critical temperatures $T_c = 5.10$ and 5.35 K, respectively. This discovery is very interesting because, so far, X elements are restricted to volatile and toxic pnictogens (X = P, As, Sb) rather than Ge. Furthermore, new germanium-platinum compounds $LaPt_4Ge_{12}$ and $PrPt_4Ge_{12}$ with the filled-skutterudite crystal structure have been synthesized by experimenters [49–54]. Magnetic susceptibility, specific heat, and electrical resistivity measurements indicate superconductivity in $LaPt_4Ge_{12}$ and $PrPt_4Ge_{12}$ below 8.3 K [49]. Moreover, $LaPt_4Ge_{12}$ has been confirmed to be a conventional Bardeen-Cooper-Schrieffer (BCS)-type superconductor by nuclear magnetic resonance (NMR) measurements [50]. In 2010, Kanetake and co-workers [55] reported on the superconducting characteristics of the filled skutterudites $LaPt_4Ge_{12}$ ($T_c = 8.3$ K) and $PrPt_4Ge_{12}$ ($T_c = 7.9$ K) by ^{73}Ge nuclear quadrupole resonance (NQR) at zero field. This experimental work indicates that one possible reason for the comparable critical transition temperatures for La and Pr compounds, which are higher than those of other MPt_4Ge_{12} (M = Sr, Ba) compounds, is their larger density of states at the Fermi level. Very recently, Chandra and co-workers [56] presented the temperature (T) and magnetic field (H) dependence of heat capacity (C) of the superconducting skutterudite compounds $LaPt_4Ge_{12}$ and $PrPt_4Ge_{12}$ along with their electronic band structures. This study shows that the zero-field $C(T)$ in the superconducting state of both the compounds can only be explained in terms of two superconducting gaps.

Although there has been a wealth of experimental works presented in recent years on structural and superconducting properties of filled-skutterudite superconductors, less attention has been paid to the theoretical side. Calculations based on the local density approximation (LDA) and full potential linearized augmented plane-wave (FP-LAPW) method have been performed to investigate the electronic properties of $LaRu_4P_{12}$ [57,58]. These theoretical works indicated that the density of states at the Fermi level is dominated by P p and Ru d states. The projector augmented-wave (PAW) method has been used to investigate the electronic properties of $BaPt_4Ge_{12}$, $LaPt_4Ge_{12}$, and $ThPt_4Ge_{12}$ by Chen [59]. This theoretical work shows that the relativistic effect has little influence on the density of states around the Fermi level for these Ge-based skutterudites [59]. Recently, the electronic properties of $LaRu_4X_{12}$ (X = P, As, Sb) were also studied by the FP-LAPW method [60]. This theoretical work, based on the generalized approximation of Perdew, Burke, and Ernzerhof [61], reveals the major contribution at the Fermi level to be mainly from X p and Ru d states. Furthermore, Ram

and co-workers [60] found no significant change in the vicinity of the Fermi level by including spin-orbit coupling (SOC). The FP-LAPW method has been also used to study the electronic properties of $LaPt_4Ge_{12}$ [56]. The results on the total density of states of $LaPt_4Ge_{12}$ are similar to that reported in the theoretical work of Gumeniuk and co-workers [49]. In addition to the electronic properties of filled-skutterudite superconductors, their vibrational properties must be also studied because many measurable properties of metals originate from the nonadiabatic coupling between electrons and phonons. Thus, the Raman-scattering technique [62–64] has been used to measure Raman active phonon modes of $LaRu_4P_{12}$. Chen [59] used a first-principles lattice dynamics method to calculate the phonon dispersion curves for $BaPt_4Ge_{12}$, $LaPt_4Ge_{12}$, and $ThPt_4Ge_{12}$. The calculated phonon dispersion curves for these materials indicate that these Ge-based skutterudites are dynamically stable [59]. Furthermore, Koza and co-workers [65] reported on the vibrational properties of the lanthanum filled skutterudites $LaRu_4Sb_{12}$, $LaOs_4Sb_{12}$, and $LaOs_4As_{12}$ investigated by inelastic neutron scattering. *Ab initio* lattice dynamical calculations by Koza and co-workers [65] were also used to obtain phonon dispersion curves and phonon density of states for these lanthanum filled-skutterudite compounds. Their theoretical work [65] indicated that these lanthanum filled-skutterudite compounds are dynamically stable since all phonon modes in these materials have real frequencies and there are no phonon branches with dispersions that dip towards the zero frequency.

To be able to understand the origin of superconductivity in the lanthanum filled-skutterudite compounds within the conventional BCS [66] theory of superconductivity, one needs to know the electron-phonon interaction in these compounds. Keeping this in mind, in this work we have employed the *ab initio* plane-wave pseudopotential calculations to study the structural, elastic, electronic, and vibrational properties, and the electron-phonon interaction in the lanthanum filled-skutterudite compounds $LaRu_4As_{12}$, $LaRu_4P_{12}$, and $LaPt_4Ge_{12}$. The electronic band structures for all the studied compounds close to the Fermi energy are analyzed and discussed in detail. A linear response theory [67] has been used to obtain the phonon dispersion relations and density of states for these compounds. The calculated zone-center phonon modes for $LaRu_4As_{12}$ are compared with previous *ab initio* results [65]. The electron-phonon matrix elements for all the studied compounds have been determined by using the linear response method and the Migdal-Eliashberg approach [68,69]. The phonon dispersion curves and the electron-phonon matrix elements have been utilized to calculate the Eliashberg spectral functions for these compounds, from which the electron-phonon coupling parameter and the logarithmic average of phonon frequency can be determined. Using the electron-phonon coupling parameter and the logarithmic average of phonon frequency, we obtain the superconducting transition temperatures of these lanthanum filled-skutterudite compounds.

II. COMPUTATIONAL DETAILS

The calculations have been made using a first-principles pseudopotential method based on density functional theory with the electronic structure package QUANTUM ESPRESSO [67]. The electronic exchange-correlation energy is estimated according to the generalized gradient approximation (GGA) of Perdew, Burke, and Ernzerhof (PBE) [61]. The electron-ion interaction is described by using norm-conserving pseudopotentials [70]. The Kohn-Sham equations [71] are solved using an iterative conjugate gradient scheme to determine total energy. Reciprocal space integration is made with sets of special points obtained by using the standard special **k**-points technique of Monkhorst and Pack [72]. For structural properties, the Brillouin zone integration has been performed using an $8 \times 8 \times 8$ **k** mesh while a $24 \times 24 \times 24$ **k**-point mesh is used for electronic properties.

The *ab initio* pseudopotential method permits total energy calculations to be made for arbitrary crystal structures. Thus, we can apply small strains to the equilibrium lattice, then determine the resulting change in the total energy, and using this information deduce the second-order elastic constants. The elastic constants can be identified as proportional to the second-order coefficient in a polynomial fit of the total energy as a function of the distortion parameter δ. There are three independent elastic constants for a cubic material, called C_{11}, C_{12}, and C_{44}. Thus, three equations are needed to calculate these elastic constants. In the direct determination of the bulk modulus, the energy versus volume curve is fitted to the Murnaghan equation of state [73]. The bulk modulus for a cubic crystal is also related to the elastic constants C_{11} and C_{12} as

$$B = \frac{(C_{11} + 2C_{12})}{3}. \tag{1}$$

For the calculation of the tetragonal shear modulus $C_{11} - C_{12}$, we use a volume-conserving tetragonal strain [74]

$$\mathbf{e} = \big(\delta,\delta,(1+\delta)^{-2} - 1,0,0,0\big). \tag{2}$$

The energy associated with such a distortion can be written as

$$E(\delta) = E(O) + 3V_O(C_{11} - C_{12})\delta^2 + O(\delta^3), \tag{3}$$

where $E(O)$ is the unstrained energy and V_O is the volume of the unit cell which remains constant. The relationship between $E - E(O)$ and δ^2 from Eq. (3) gives the shear modulus $C_{11} - C_{12}$. The elastic constants C_{44} can be calculated by the distortion of the lattice using the volume-conserving distortion [74]

$$e = \left(0,0,\frac{\delta^2}{(4-\delta^2)},0,0,\delta\right). \tag{4}$$

The energy associated with this distortion is

$$E = E(O) + \tfrac{1}{2}C_{44}V_O\delta^2 + O(\delta^4). \tag{5}$$

The elastic constant C_{44} can be directly obtained from the above equation. The elastic constants C_{11} and C_{12} can be calculated by combining the tetragonal shear modulus with the relation for the bulk modulus in Eq. (1). The calculations of the elastic constants need a very high degree of precision because the energy differences involved are on the order of less than 1 mRy. To ensure this requires the use of a fine ***k***-point mesh. With our choice of a $16 \times 16 \times 16$ **k**-points grid the energy per atom is converged to 1 mRy or better in all cases. In this study, we have calculated a set of 21 values

of $\frac{E(\delta)-E(0)}{V_o} - \delta$ by varying δ from -0.02 to 0.02 in steps of 0.002. Then, we have fitted these results to a parabola, and the elastic constants are calculated from the quadratic coefficients. The calculated elastic constants can be used to obtain the Hill [75] shear modulus G_H, which is the arithmetic mean of the Voigt [76] and Reuss [77] approximations. In addition, the Debye temperature can be determined by means of the mean sound velocity (V_m) in the following approximation [78]:

$$\Theta_D = \frac{h}{k}\left(\frac{3n}{4\pi}\frac{N_A\rho}{M}\right)^{1/3} V_m, \tag{6}$$

where k is Boltzmann's constant, h is Planck's constant, n is the number of atoms in the molecule, N_A is Avogadro's number, ρ denotes the mass density, and M is the molecular weight. The mean sound velocity can be given as

$$V_m = \left[\frac{1}{3}\left(\frac{2}{V_T^3} + \frac{1}{V_L^3}\right)\right]^{-1/3}, \tag{7}$$

$$V_T = \left(\frac{G_H}{\rho}\right)^{1/2}, \tag{8}$$

$$V_L = \left(\frac{3B + 4G_H}{3\rho}\right)^{1/2}, \tag{9}$$

where V_T and V_L are transverse and longitudinal sound velocities, respectively.

After achieving self-consistent solutions of the Kohn-Sham equations, the vibrational properties (the phonon spectrum, the density of states, and the eigenvectors corresponding to phonon frequencies) have been calculated within the framework of the self-consistent density functional perturbation theory [67]. We have calculated eight dynamical matrices for a $4 \times 4 \times 4$ **q**-point mesh within the irreducible part of the Brillouin zone. The dynamical matrices at arbitrary wave vectors can be evaluated by means of a Fourier deconvolution on this mesh. The superconducting properties have been studied using the phonon-mediated coupling Migdal-Eliashberg [68,69] theory based on the BCS model [66]. The main quantity in the Migdal-Eliashberg [68,69] theory is the electron-phonon spectral function, which is given as [79]

$$\alpha^2 F(\omega) = \frac{1}{2\pi N(E_F)} \sum_{\mathbf{q}j} \frac{\gamma_{\mathbf{q}j}}{\hbar\omega_{\mathbf{q}j}} \delta(\omega - \omega_{\mathbf{q}j}), \tag{10}$$

where $N(E_F)$ presents the electronic density of states per atom and spin at the Fermi level. When the electron energies around the Fermi level are linear in the range of phonon energies, the phonon linewidth is given by Fermi's golden rule formula [79]:

$$\gamma_{\boldsymbol{q}j} = 2\pi\omega_{\boldsymbol{q}j} \sum_{knm} \left|g^{\boldsymbol{q}j}_{(\boldsymbol{k}+\boldsymbol{q})m;\boldsymbol{k}n}\right|^2 \delta(\varepsilon_{\boldsymbol{k}n} - \varepsilon_F)\delta(\varepsilon_{(\boldsymbol{k}+\boldsymbol{q})m} - \varepsilon_F), \tag{11}$$

where the Dirac delta functions express energy-conservation conditions. The matrix element for electron-phonon interaction is [79]

$$g^{\mathbf{q}j}_{(\mathbf{k}+\mathbf{q})m;\mathbf{k}n} = \sqrt{\frac{\hbar}{2M\omega_{\mathbf{q}j}}} \langle\phi_{(\mathbf{k}+\mathbf{q})m}|\mathbf{e}_{\mathbf{q}j} \cdot \vec{\nabla} V^{\mathrm{SCF}}(\mathbf{q})|\phi_{\mathbf{k}n}\rangle, \tag{12}$$

where M is atomic mass and $\vec{\nabla} V^{\mathrm{SCF}}(\mathbf{q})$ is the derivative of the self-consistent effective potential with respect to the atomic displacement caused by a phonon with wave vector $\boldsymbol{q}$. From $\alpha^2 F(\omega)$, we can obtain λ, which is a good measure of the overall strength of the electron-phonon interaction; it is given by

$$\lambda = 2\int \frac{\alpha^2 F(\omega)}{\omega} d\omega. \tag{13}$$

The Allen-Dynes modified McMillan equation [79] can be used to determine the superconducting critical temperature T_c,

$$T_c = \frac{\omega_{\ln}}{1.2} \exp\left(-\frac{1.04(1+\lambda)}{\lambda - \mu^*(1+0.62\lambda)}\right), \tag{14}$$

where μ^* is a Coulomb pseudopotential which takes values between 0.10 and 0.16 [79]. In our calculations, we have decided to use the average of these limiting values, i.e., $\mu = 0.13$. In this work, the logarithmically averaged frequency $\omega_{\ln}$ is calculated from [79]

$$\omega_{\ln} = \exp\left(\frac{1}{\lambda}\sum_{\boldsymbol{q}j} \lambda_{\boldsymbol{q}j} \ln\omega_{\boldsymbol{q}j}\right). \tag{15}$$

III. RESULTS

A. Structural, elastic, and electronic properties

Ternary intermetallic compounds LnT_4X_{12} (Ln = La; T = Ru, Pt; X = P, As, Ge) crystallize in the $CoAs_3$-type skutterudite structure filled by La atoms, as shown in Fig. 1. This structure is body-centered cubic (bcc) with space group $Im\bar{3}$. The atomic positions are for 1 La atom in (2a) (0, 0, 0); for 4 T atoms in (8c) (1/4, 1/4, 1/4); and for 12 X atoms in (24g) $(0, y, z)$, where y and z are the so-called internal parameters. These internal parameters determine the relative positions of X atoms in the $[T_4X_{12}]$ polyanion.

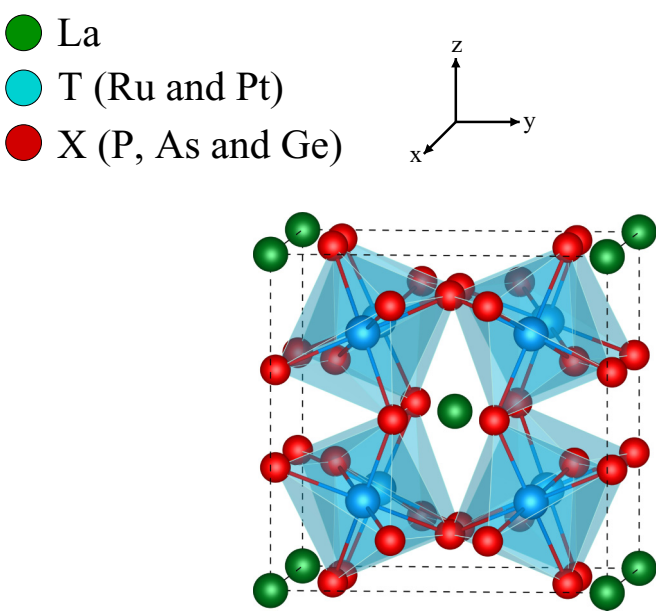

FIG. 1. The body-centered cubic structure of the filled skutterudites $LaRu_4P_{12}$, $LaRu_4As_{12}$, and $LaPt_4Ge_{12}$.

TABLE I. Structural properties of the body-centered cubic $LaRu_4P_{12}$, $LaRu_4As_{12}$, and $LaPt_4Ge_{12}$ and their comparison with previous experimental and theoretical results.

Material	a (Å)	V (Å^3)	y	z	B (GPa)	B'
$LaRu_4P_{12}$	8.1227	267.96	0.3588	0.1436	160	4.40
Experiment [45]	8.060	261.85			172	
GGA [60]			0.3577	0.1444		
Experiment [37]	8.0561	261.42				
Experiment [18]	8.0610	261.90	0.3591	0.1428		
Experiment [39]	8.0516	260.98				
$LaRu_4As_{12}$	8.6254	320.85	0.3499	0.1502	122	4.46
Experiment [38]	8.5097	308.11				
Experiment [39]	8.5081	307.94				
Experiment [60]			0.3500	0.1470		
GGA [60]			0.3501	0.1503		
GGA [65]	8.6074	318.8	0.3497	0.1508	115	
$LaPt_4Ge_{12}$	8.7683	337.07	0.3550	0.1510	100	4.75
Experiment [51]	8.6235	320.64	0.3549	0.1517		
Experiment [55]	8.618	320.03				
GGA [59]	8.750	334.96				

As a consequence, the structure of these lanthanum filled skutterudites is defined by one lattice parameter (a) and two internal structural parameters (y and z). To start with, the structural optimization calculations for these lanthanum filled skutterudites have been performed using the total energy minimization and zero atomic force criteria. Thus, we are able to identify the equilibrium values of lattice and internal parameters for all the considered materials. For determining their bulk modulus and the pressure derivative of bulk modulus, the total energy is calculated as a function of volume and fitted to the Murnaghan equation of state [73]. The calculated equilibrium lattice constant (a), the equilibrium volume (V), the internal parameters y and z, the bulk modulus (B), and its pressure derivative (B') are presented and compared with previous experimental [18,37–39,45,51,55,60] and theoretical results [59,60,65] in Table I. As can be seen from this table, the replacement of P by the larger As and Ge atoms gives rise to lengthening of the lattice parameter in $LaRu_4P_{12}$ and $LaPt_4Ge_{12}$. The maximum difference between the calculated and experimental lattice parameters is found to be around 2% while the calculated internal parameters are very close to their experimental values [18,37–39,45,51,55,60]. The calculated bulk modulus of $LaRu_4P_{12}$ is comparable with its experimental value [45] of 172 GPa. We note that experimental data do not exist for the bulk modulus of the remaining lanthanum filled skutterudites.

In the body-centered cubic structure of the filled skutterudites $LaRu_4P_{12}$, $LaRu_4As_{12}$, and $LaPt_4Ge_{12}$, La filler atoms constitute the electropositive cations and give valence electrons to the transition metal–X network. In the resulting polyanions, the transition-metal atoms reside in the center of a distorted octahedral environment of six X atoms. The spatial coordination of these octahedra in the unit cell causes generation of huge empty icosahedral spaces in the framework structure, which are filled by La atoms. As a result, we can conclude that the role of the La filler atom as its electron donor function is primary a geometric one. Thus, the electropositive La atoms and the $[T_4X_{12}]$ polyanions are bonded together due to ionic interactions. The atomic distance within the $[T_4X_{12}]$ polyanion is found to be slightly shorter than the sum of the corresponding atomic radii. For example, the bond length between Pt and Ge atoms is calculated to be 2.53 Å, which is considerably smaller than the sum of the atomic radii ($R^{\mathrm{Pt}} = 1.35$ Å and $R^{\mathrm{Ge}} = 1.25$ Å) and thus confirms strong covalent Pt-Ge bonding within the $[Pt_4Ge_{12}]$ polyanion. As a consequence, the bonding in these lanthanum filled skutterudites is primarily of covalent-ionic nature with the existence of some metallic character.

The elastic properties of solids must be studied because they constitute a bridge between the mechanical and vibrational properties. Thus, they must affect the superconducting properties of solids since phonons play the role of bringing about the coupling together of two electrons to form Cooper pairs in the phonon-mediated version of the BCS theory. Furthermore, they give information on the stability and stiffness of solids. The calculated values of C_{11}, C_{12}, C_{44}, G_H, V_T, V_L, and Θ_D are given in Table II. It is well established that for mechanical stability of cubic crystals their independent elastic constants must obey Born's criteria [80]: $C_{11} > C_{12}$, $C_{44} > 0$, and $C_{11} + 2C_{12} > 0$. The elastic constants of all the studied compounds satisfy Born's criteria [80], which confirms that these materials are mechanically stable. Unfortunately, no experimental measurements of the elastic constants of all the

TABLE II. Elastic constants (C_{11}, C_{12}, and C_{44}), Hill's shear modulus (G_H), transverse and longitudinal acoustic speeds V_T and V_L, and Debye temperature (Θ_D) for the body-centered cubic $LaRu_4P_{12}$, $LaRu_4As_{12}$, and $LaPt_4Ge_{12}$ and their comparison with previous experimental and theoretical results.

Material	C_{11} (GPa)	C_{12} (GPa)	C_{44} (GPa)	G_H (GPa)	V_T (m/s)	V_L (m/s)	Θ_D (K)
$LaRu_4P_{12}$	288	95	111	105	4306	7267	566
Experiment [44]							603
Experiment [38]							446
$LaRu_4As_{12}$	235	66	62	70	3089	5360	383
GGA [65]	242	52	64	75	3235	5446	388
Experiment [44]							355
Experiment [38]							233
Experiment [46]							388
$LaPt_4Ge_{12}$	146	77	9	16	1343	3708	168
Experiment [49]							209

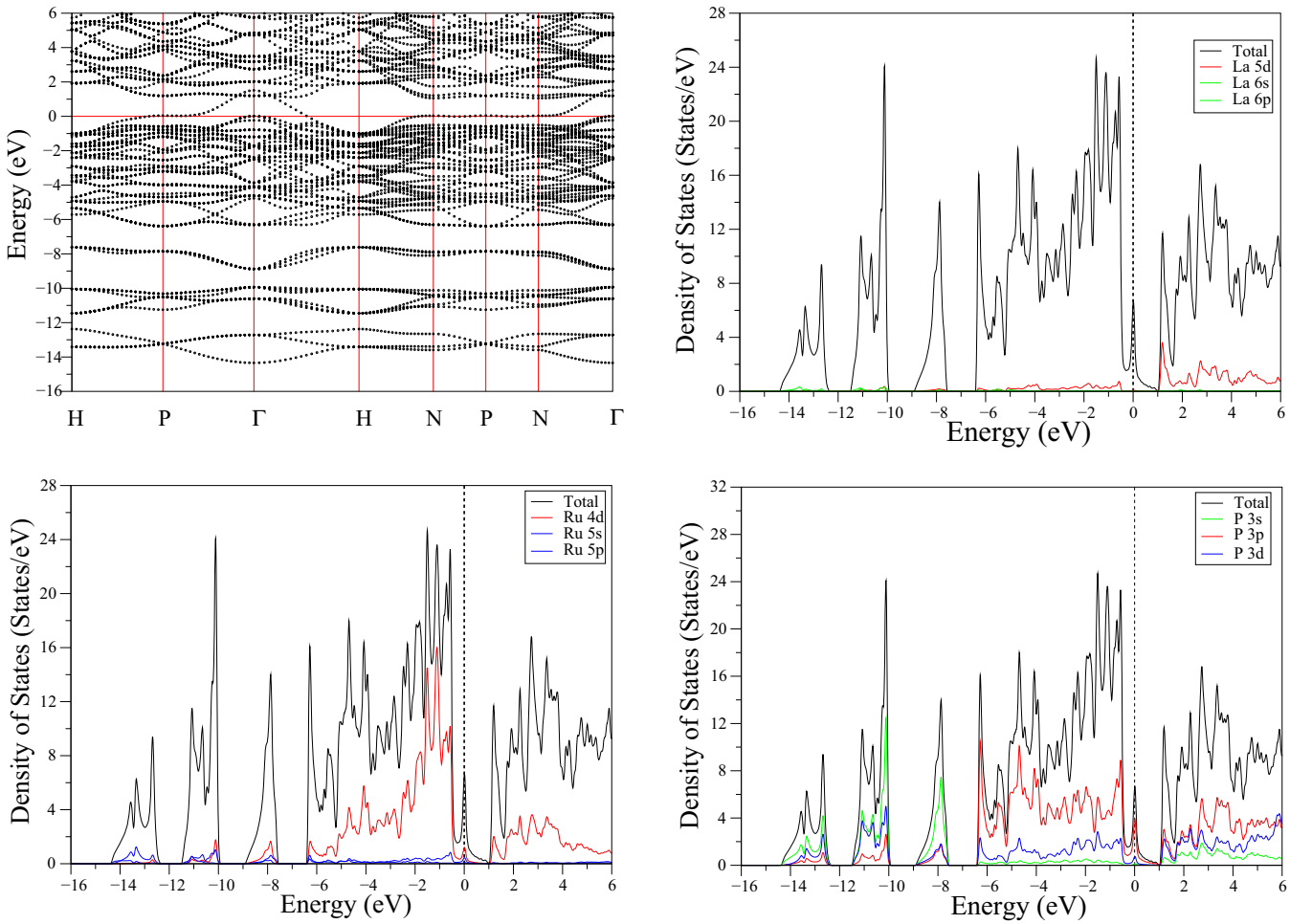

FIG. 2. The electronic band structure for $LaRu_4P_{12}$ along symmetry directions of the body-centered-cubic zone. Total and partial electronic density of states for $LaRu_4P_{12}$. Fermi level is fixed to 0 eV.

considered materials have been reported yet. However, our calculated elastic constants for $LaRu_4As_{12}$ agree very well with previous GGA calculations [65]. Furthermore, the calculated Debye temperatures of all studied materials are comparable with their corresponding experimental results [38,44,46,49]. These two results indicate that our elastic results for all the considered materials should show good agreement with any future measurements. Pugh [81] suggested a simple relationship in which the ductile and brittle properties of compounds should be associated empirically to their elastic constants by the ratio G_H/B. If this ratio is smaller than 0.57 ($G_H/B < 0.57$), the compounds behave in a ductile manner and brittle otherwise. The values of this ratio are found to be 0.65 for $LaRu_4P_{12}$, 0.57 for $LaRu_4As_{12}$, and 0.16 for $LaPt_4Ge_{12}$. From these results, we can state that $LaPt_4Ge_{12}$ behaves in a ductile manner while $LaRu_4P_{12}$ behaves in a brittle manner. However, the value of this ratio for $LaRu_4As_{12}$ is equal to the critical value (0.57) separating ductile and brittle materials. Now, we can conclude that from the point of applications, $LaPt_4Ge_{12}$ is more appealing.

Figure 2 depicts the calculated energy-band structure of $LaRu_4P_{12}$ along selected high-symmetry directions within the body-centered-cubic first Brillouin zone. The calculated band structure for $LaRu_4P_{12}$ is consistent with previous theoretical studies [57,58,60]. The dispersive band crosses the Fermi level along the Γ-N and Γ-H directions, showing the metallic nature of $LaRu_4P_{12}$. The Fermi level coincides with the band along the flat band along N-P. This flat feature leads to a peak in the density of states and hence gives rise to an enhancement of the superconductivity feature in $LaRu_4P_{12}$. To identify the specific electronic states connected with superconductivity, the total and partial density of states (PDOS) are examined in detail (see Fig. 2). The deep-lying bands below −6.4 eV mainly arise from the *s* states of P atoms but a measurable contribution of P *p* and *d* orbitals is also present. The main valence-band region of $LaRu_4P_{12}$ extends from −6.4 eV to the Fermi level. The PDOS of Pt and Ge considerably appear in the energy range below and above the Fermi level. In particular, at energy values from −6.4 to −4.0 eV, the density of states (DOS) features are mainly dominated by the *p* states of P atoms. In contrast, the contribution of the La filler atoms to the valence bands is very small while the PDOS of La exist almost only above the Fermi level. This picture suggests that the bonding nature of $LaRu_4P_{12}$ can be described as an electron transfer from the La filler atoms to the $[Ru_4P_{12}]$ polyanion. Thus, the valence DOS region of $LaRu_4P_{12}$ is mainly dominated by the states of the $[Ru_4P_{12}]$ polyanion. In particular, the intensity patterns of the PDOS of Ru and P atoms resemble each other, confirming

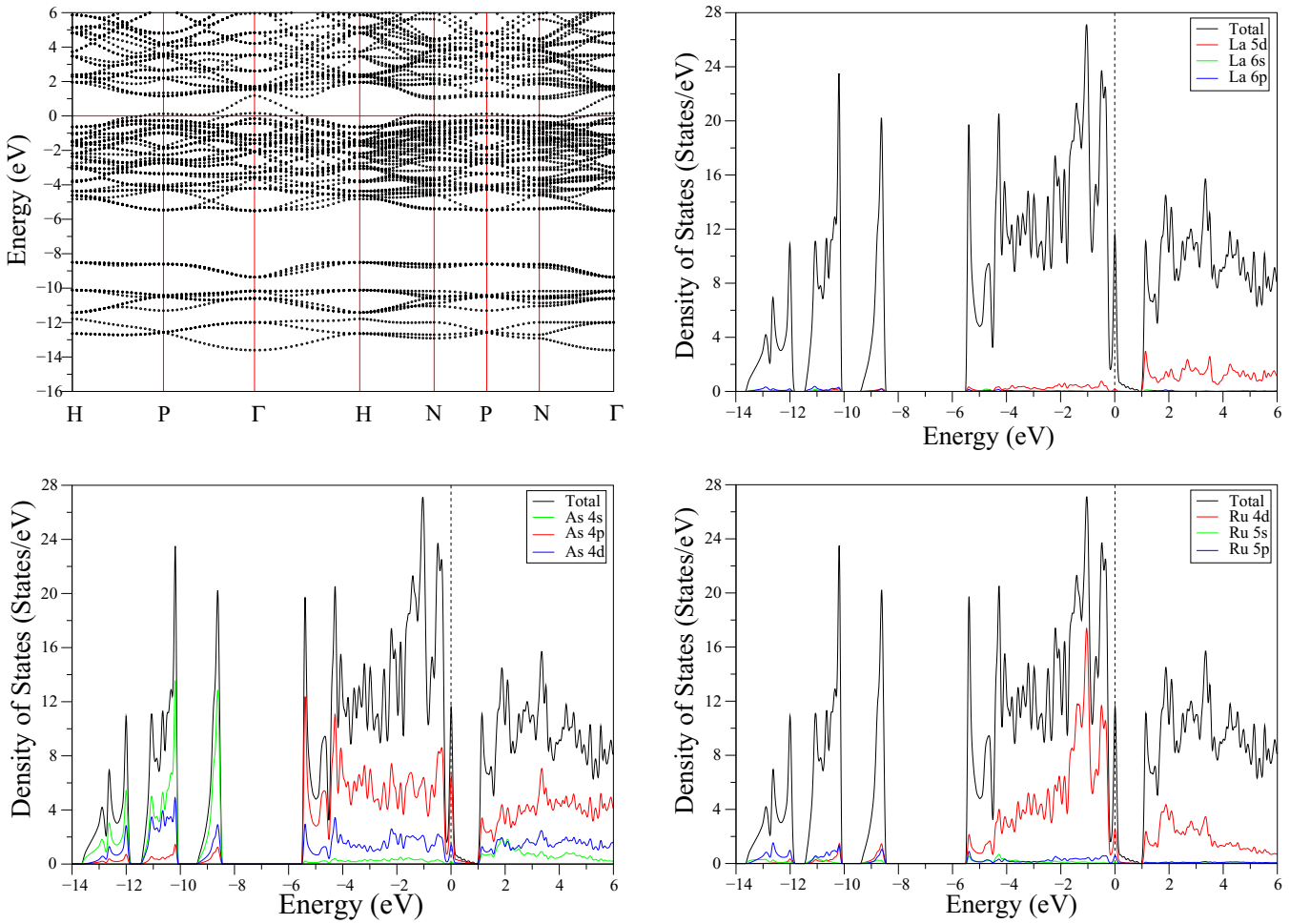

FIG. 3. The electronic band structure for $LaRu_4As_{12}$ along symmetry directions of the body-centered-cubic zone. Total and partial electronic density of states for $LaRu_4As_{12}$. Fermi level is fixed to 0 eV.

the Ru and P orbitals hybridize over the wide energy range around the Fermi level. Since electrons near the Fermi level are involved in the generation of the superconducting state, their nature must be analyzed in detail. The DOS in the vicinity of the Fermi level is contributed by the p states of P atoms with considerable admixture of Ru d states. The Fermi level that lies on a sharply increasing peak with an energy of 0.008 eV is mainly made up from P p states due the flat band along the N-P direction (see Fig. 2). This picture is crucial for superconductivity in $LaRu_4P_{12}$ because Cooper pairs in BCS theory can be constituted by electrons which have energies close to the Fermi level. The density of states at the Fermi level $[N(E_F)]$ for $LaRu_4P_{12}$ amounts to be 6.70 states/eV which is comparable with the corresponding experimental value of 7.14 states/eV [38]. The orbital analysis of the DOS shows that primarily La (2%), Ru (26%), and P (72%) electronic states are contributing to the value of $N(E_F)$. This result indicates that the influence of La filler atoms on superconductivity can be ignored while the observed superconductivity in $LaRu_4P_{12}$ seems to be an intrinsic feature of the $[Ru_4P_{12}]$ polyanion.

The electronic band structure and total and partial density of states for $LaRu_4As_{12}$ are displayed in Fig. 3. The overall band profile is in good agreement with previous theoretical results [60]. Comparison of the band structure and DOS shapes for $LaRu_4As_{12}$ and $LaRu_4P_{12}$ indicates that the common features of their electronic spectra are very similar to each other. This result is expected because these materials are isostructural as well as isoelectronic to each other. However, the main valence-band region of $LaRu_4As_{12}$ is 0.9 eV smaller than the corresponding region of $LaRu_4P_{12}$. Thus, As p states and Ru d states hybridize more strongly than P p and Ru d states. Thus, when P is replaced by As, the value of $N(E_F)$ increases from 6.70 to 11.19 states/eV. The enhancement in the value of $N(E_F)$ for $LaRu_4As_{12}$ as compared to that for $LaRu_4P_{12}$ is expected to lead to the increase in the value of T_c of this material according to the McMillan-Hopfield expression,

$$\lambda = \frac{N(E_F)\langle I^2\rangle}{M\langle\omega^2\rangle}, \tag{16}$$

where $\langle I^2\rangle$ denotes the averaged square of the electron-phonon matrix element, $\langle\omega^2\rangle$ is the averaged square of the phonon frequency, and M is the mass involved. This expression shows that the rise in the value of $N(E_F)$ will increase the value of the electron-phonon coupling parameter (λ), which makes a positive contribution to the value of T_c.

The electronic band structure and total and partial density of states for $LaPt_4Ge_{12}$ are illustrated in Fig. 4. The overall

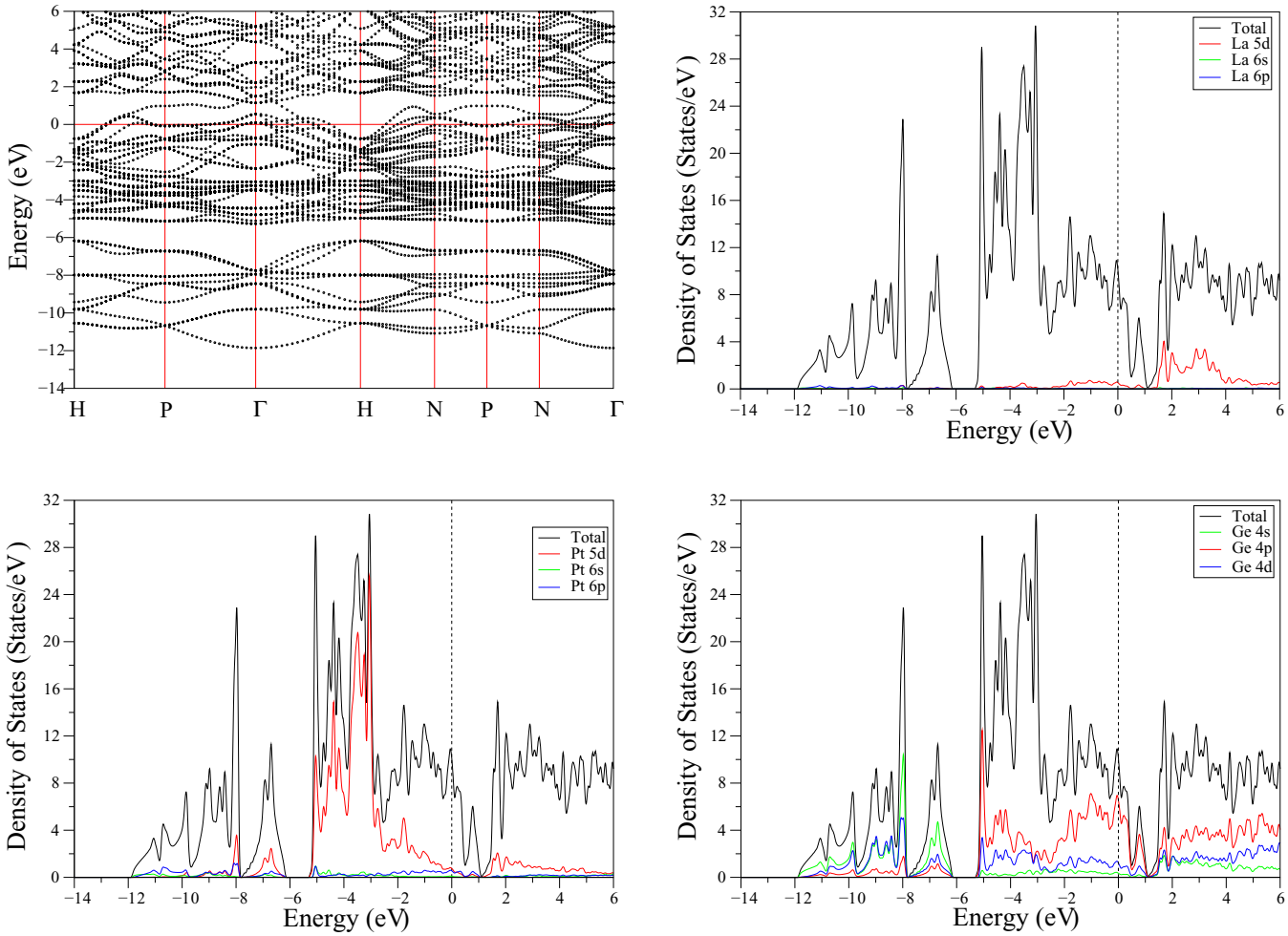

FIG. 4. The electronic band structure for $LaPt_4Ge_{12}$ along symmetry directions of the body-centered-cubic zone. Total and partial electronic density of states for $LaPt_4Ge_{12}$. Fermi level is fixed to 0 eV.

band profile is in good agreement with previous theoretical results [59]. Again the contribution of La electronic states to the valence bands is very small, while the PDOS of Pt and Ge are widely distributed in the energy range below and above the Fermi level. In particular, the low-lying valence bands mainly originate from the mixture of Ge electronic states, while the DOS features between -5.3 and -3.0 eV are dominated by the d states of Pt atoms, which hybridize strongly with the p states of Ge atoms. The valence bands close to the Fermi level are mainly contributed by the p states of Ge atoms with smaller contributions coming from the d states of remaining atoms. Again, the Fermi level lies on a sharply increasing peak for $LaPt_4Ge_{12}$, giving rise to a high density of states at the Fermi level [$N(E_F) = 9.60$ states/eV], but is smaller than the corresponding value of 11.19 states/eV for $LaRu_4As_{12}$. This decrease can be linked to the decrease in the contribution of transition-metal atoms to the value of $N(E_F)$ for $LaPt_4Ge_{12}$. Finally, we have to mention that the largest contribution to $N(E_F)$ comes from Ge atoms with around 80%. This result indicates that Ge p states are able to greatly influence the electronic and superconducting properties of $LaPt_4Ge_{12}$.

It should be pointed out that the sharpness of the DOS at the Fermi level and the magnitude of the DOS at the Fermi level [$N(E_F)$] change rather sensitively with the broadening factor in evaluating the DOS, but more so for the As- and P-containing compounds than the Ge compounds. This indicates that the Fermi surface topology, electron-phonon coupling parameter (λ), and T_c are subject to perturbation more sensitively for $X =$ As and P than for $X =$ Ge. The theoretical work in Ref. [60] reported changes in the Fermi surface topology for As- and Sb-containing compounds under compression. However, we are not aware of any experimental reports for the susceptibility of these parameters to the relative sensitivities against perturbations for $X =$ As and P, compared to that for $X =$ Ge. It would be useful to perform experiments for these materials under pressure to examine such features.

B. Phonons and electron-phonon interaction

Since the primitive unit cell of all the studied materials is composed of 17 atoms, there are 51 phonon branches, containing 3 acoustic branches and 48 optical branches. The zone-center optical phonon modes of lanthanum filled-skutterudite compounds are classified by the irreducible representation of the point group T_h ($m\bar{3}$). As deduced from group theory, the symmetries of the optical phonon modes are presented as

$$\Gamma = 8T_u(I) + 2E_u + 2A_u + 4T_g(R) + 2E_g(R) + 2A_g(R),$$

TABLE III. The zone-center phonon modes (in THz) of $LaRu_4As_{12}$, $LaRu_4P_{12}$, and $LaPt_4Ge_{12}$ superconductors. Previous theoretical results for $LaRu_4As_{12}$ [65] and Raman results for $LaRu_4P_{12}$ [62,64] are shown in parentheses.

Mode	$LaRu_4As_{12}$	$LaRu_4P_{12}$	$LaPt_4Ge_{12}$
T_u (I)	1.78 (1.95)	2.89	1.80
	3.49 (3.41)	5.51	2.25
	4.40 (4.34)	6.08	2.58
	5.58 (5.58)	7.17	3.68
	5.96 (5.96)	8.10	4.02
	6.84 (6.83)	9.71	5.04
	7.02 (7.09)	11.38	5.99
	7.66 (7.73)	12.32	6.25
E_u	4.73 (4.67)	6.07	2.65
	7.52 (7.60)	10.79	6.18
A_u	3.19 (3.44)	5.07	1.57
	6.83 (7.01)	10.29	5.65
T_g (R)	3.79 (3.80)	7.25	2.47
	4.50 (4.62)	8.76	3.14
	6.13 (6.25)	10.03	5.17
	7.25 (7.44)	11.69	5.76
E_g (R)	5.59 (5.59)	10.30 (10.91)	3.93
	6.77 (6.17)	12.23 (12.83)	5.93
A_g (R)	6.29 (6.23)	10.20	5.02
	6.88 (6.79)	12.64 (13.21)	6.56

where A, E, and T are singly, doubly, and triply degenerate modes, respectively. R and I correspond to Raman and infrared active phonon modes. The calculated zone-center optical phonon modes for all the studied compounds are presented in Table III, together with previous theoretical results [65] for $LaRu_4As_{12}$ and Raman results [62,64] for $LaRu_4P_{12}$. First, as it is expected, the zone-center phonon modes in $LaRu_4P_{12}$ have higher frequencies than their counterparts in the remaining materials due to its smaller lattice constant and smaller total masses as compared to the lattice constants and total masses of the remaining materials. Second, the calculated results for $LaRu_4As_{12}$ are consistent with previous theoretical calculations [65]. In particular, the maximum difference in the result in Ref. [65] and our work, found for the second E_g phonon mode of $LaRu_4As_{12}$, is around 9%. Third, the frequencies of two E_g (10.30 and 12.23 THz) and highest A_g (12.64) modes for $LaRu_4P_{12}$ compare very well with their experimental values of 10.91, 12.83, and 13.21 THz [62,64].

The calculated phonon spectra along the high symmetry lines of the body-centered-cubic Brillouin zone, together with total and partial phonon DOS, for $LaRu_4P_{12}$ are depicted in Fig. 5. The phonon frequency spectrum is separated into three distinct regions with two narrow gaps of 0.5 and 0.3 THz due to the large mass difference between La (or Ru) and P atoms. The first frequency region contains a set of 24 phonon branches extending up to 8.3 THz. Three acoustic phonon branches disperse up to 3.0 THz while the optical phonon modes lie between 3.0 and 8.3 THz. The remaining 51 phonon branches lie between 9.5 and 13.6 THz. These optical phonon branches display dispersive character similar to the corresponding optical phonon branches in the first frequency

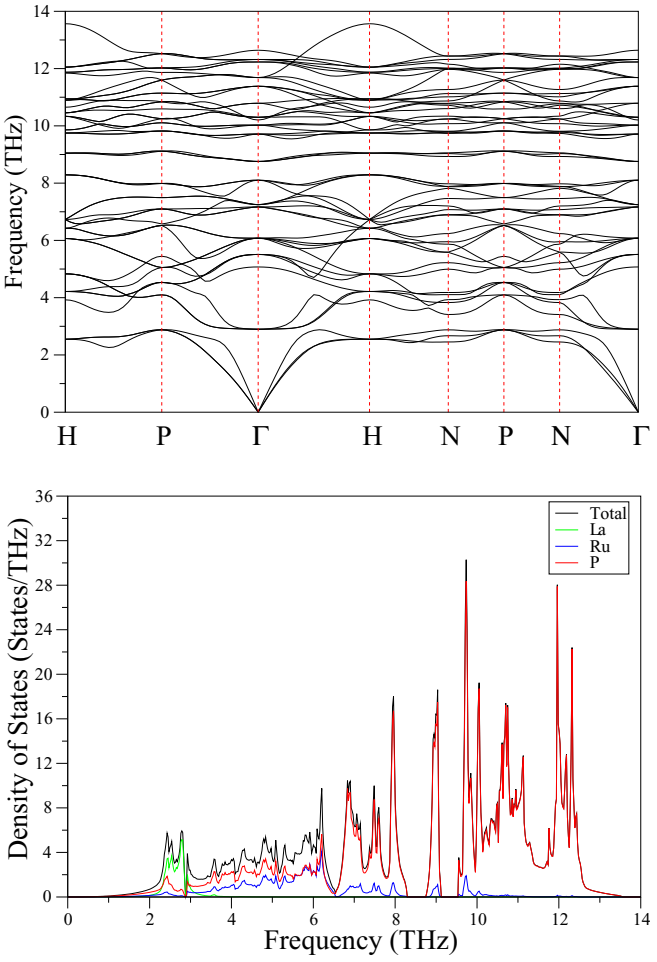

FIG. 5. Top: The phonon dispersion for $LaRu_4P_{12}$ along symmetry directions of the body-centered-cubic zone. Bottom: Total and partial phonon density of states for $LaRu_4P_{12}$.

region. The nature of phonon branches in the phonon spectrum can be explained much better by analyzing total and partial DOS in Fig. 5. Vibrational modes related to La atoms are located in the low-frequency region below 2.9 THz due to the heaviest mass of these atoms. Thus, La atoms make a contribution predominantly to three acoustic phonon branches while they seem motionless above 4 THz. However, the PDOS of the P atom is widely distributed in the whole range of phonon frequencies because its mass is much lighter than those of La and Ru atoms. In particular, a strong overlap between Ru and P vibrations appears in the frequency region from 3.5 to 6.5 THz due to the strong covalent bond between these atoms. This frequency region may be crucial for superconductivity in $LaRu_4P_{12}$ because the coupled motion of Ru and P atoms is expected to create strong electron-phonon interaction due to the considerable presence of P p and Ru d states at the Fermi level.

We present the results for the phonon dispersion curves and the corresponding DOS for $LaRu_4As_{12}$ in Fig. 6. At first glance, the phonon spectrum of $LaRu_4As_{12}$ looks different from that of $LaRu_4P_{12}$ owing to the heavier mass of As as compared to that of P. First, the total phonon spectrum of $LaRu_4As_{12}$ has a frequency range of about 8.3 THz, which is 5.3 THz smaller than that of $LaRu_4P_{12}$. Second, the 51 phonon

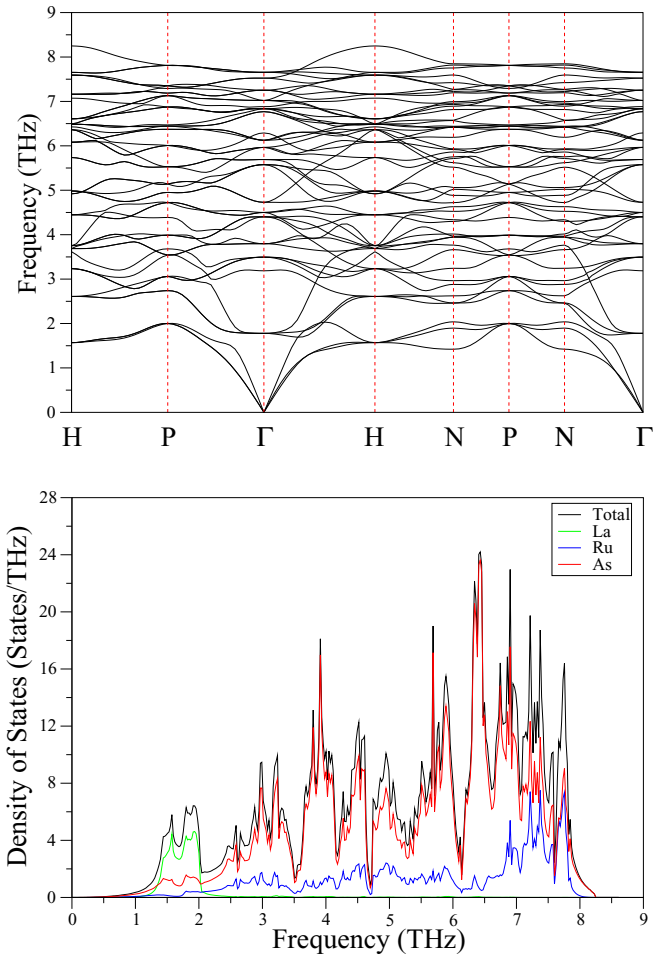

FIG. 6. Top: The phonon dispersion for $LaRu_4As_{12}$ along symmetry directions of the body-centered-cubic zone. Bottom: Total and partial phonon density of states for $LaRu_4As_{12}$.

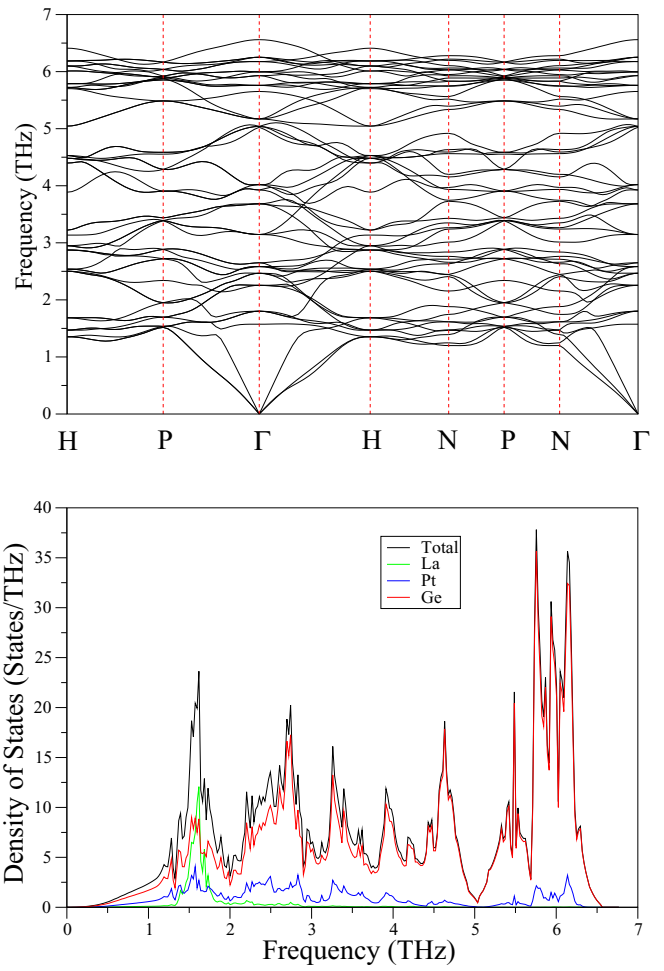

FIG. 7. Top: The phonon dispersion for $LaPt_4Ge_{12}$ along symmetry directions of the body-centered-cubic zone. Bottom: Total and partial phonon density of states for $LaPt_4Ge_{12}$.

branches fill the entire frequency range, leaving no gap in the phonon spectrum of $LaRu_4As_{12}$. Third, although the transverse and longitudinal acoustic (TA and LA) branches behave normally in the long-wave limit with steep slopes, the LA branch overlaps with two lowest-lying optical phonon branches along the Γ-H symmetry direction. Finally, different from the phonon spectrum of $LaRu_4P_{12}$, all phonon branches are quite dispersive in the phonon spectrum of $LaRu_4As_{12}$. To understand the contributions of various modes in the phonon spectrum, we now examine our results for total and partial DOS of $LaRu_4As_{12}$. Again, as expected, the vibrations of La as the heaviest element in the compound dominate the low-frequency region below 2.0 THz while its contribution vanishes above 3.0 THz. Different from $LaRu_4P_{12}$, the Ru-related phonon densities like the Ge-related phonon densities are quite dispersive, partaking in lattice vibrations over a whole range of phonon frequencies due to the smaller mass difference between Ru and As atoms as compared to the corresponding difference between Ru and P atoms. In particular, strong hybridization between Ru-related and As-related vibrations is present at the high-frequency region above 6.5 THz.

The phonon dispersion curves and the corresponding phonon DOS for $LaPt_4Ge_{12}$ are shown in Fig. 7. At first glance, the phonon spectrum of $LaPt_4Ge_{12}$ looks similar to that of $LaRu_4As_{12}$ but different from that of $LaRu_4P_{12}$. In agreement with $LaRu_4As_{12}$, all phonon branches are quite dispersive, and there is no gap in the phonon spectrum of $LaPt_4Ge_{12}$. Different from other lanthanum filled skutterudites, the salient feature of the phonon spectrum for $LaPt_4Ge_{12}$ is that the low-lying optical phonon branches strongly overlap with the acoustic phonon branches. This difference can be related to the large mass difference between Pt and Ru atoms. The phonon DOS of $LaPt_4Ge_{12}$ also exhibits some differences from those of the remaining materials. First, the contribution of Ge atoms to phonon DOS features is almost the strongest in the whole range of phonon frequencies. Second, the peak at 1.5 THz in the phonon DOS is formed by a significant La-Ge hybridization. Third, although Pt atoms are the heaviest of the three atomic types, they make considerable contribution to the DOS features up to 6.4 THz. This finding can be connected to strong bonding forces between Pt and Ge atoms. A critical assessment of electronic and phonon structures for $LaPt_4Ge_{12}$ reveals that the Ge p electrons considerably contribute to valence bands of this material, and also that Ge atoms almost dominate all phonon branches of this material. As a consequence, the Ge

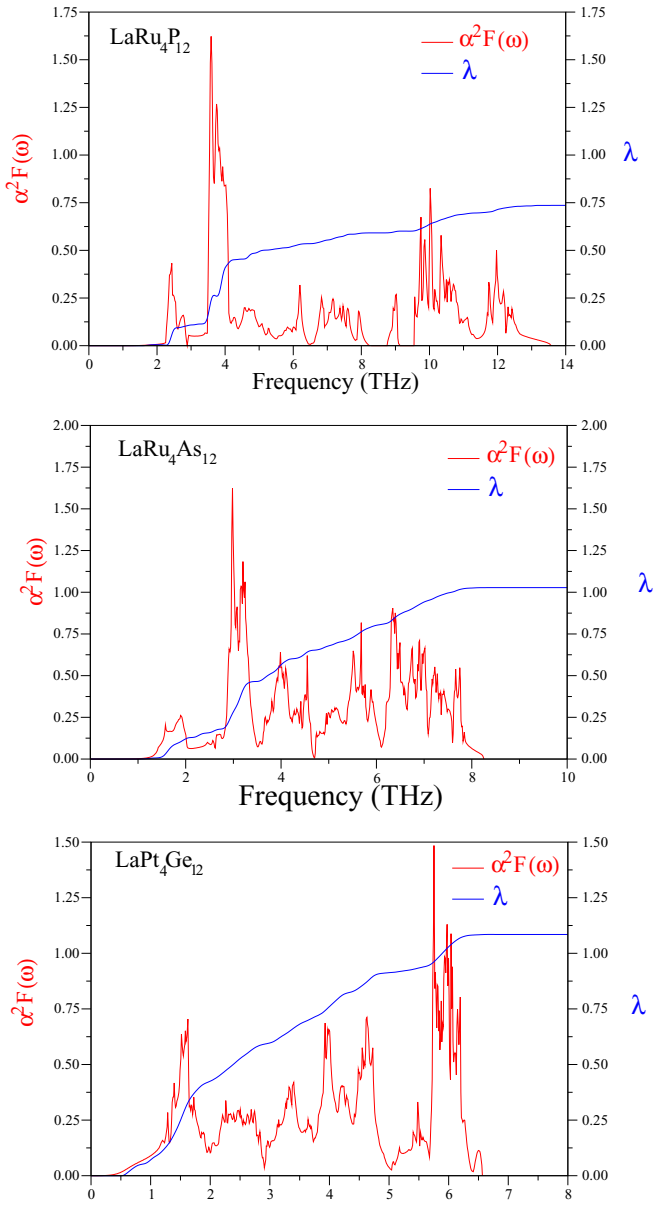

FIG. 8. The calculated electron-phonon spectral function $\alpha^2F(\omega)$ (red line) and the frequency accumulated electron-phonon coupling parameter λ (blue line) for $LaRu_4P_{12}$, $LaRu_4As_{12}$, and $LaPt_4Ge_{12}$ superconductors.

p DOS and Ge atomic vibrations play a main role in the formation of the superconducting state for $LaPt_4Ge_{12}$.

Figure 8 illustrates the Eliashberg spectral function $[\alpha^2F(\omega)]$ and the frequency accumulation of the average electron-phonon coupling parameter (λ) for all the studied materials. First, we examine the spectral function contribution to the value of λ for $LaRu_4P_{12}$. As we have mentioned before, the acoustic phonon branches of this material disperse up to 3.0 THz. These branches make a contribution of about 15% (0.11) to the value of λ while the phonon modes lying between 3.0 and 6.5 THz contribute about 62% (0.46) to the value of λ. Thus, only 23% of λ for $LaRu_4P_{12}$ is contributed by the remaining phonon modes. This smaller contribution from the frequency region above 6.0 THz can be explained by using the McMillan-Hopfield expression [see Eq. (16)]. Although the p states of P make the largest contribution to the value of $N(E_F)$, larger phonon frequencies tend to reduce the value of λ according to the McMillan-Hopfield expression [see Eq. (16)]. On the other hand, the largest contribution to λ from low-frequency optical modes is expected because they are due to the coupled motion of Ru and P atoms which dominate the electronic states near the Fermi level with their d (Ru) and p (P) states. As a consequence, low-frequency optical phonon modes in $LaRu_4P_{12}$ are more involved in the process of scattering of electrons as compared to the rest of the phonon modes.

We now examine the spectral function contribution to the value of λ for $LaRu_4As_{12}$. Different from $LaRu_4P_{12}$, the value of λ for $LaRu_4As_{12}$ increases considerably with rising phonon frequency in the whole frequency range. This means that even high-frequency phonon modes of $LaRu_4As_{12}$ are significantly involved in the process of scattering of electrons. The smallest contribution, within about 11% (0.11), to λ comes from phonon modes below 2.0 THz. This small contribution is expected since these phonon modes originate from the oscillations of La atoms. As we have mentioned before, the effect of the La filler atoms on superconductivity can be ignored because the contribution of La atoms to valence bands near the Fermi level is negligible. The phonon modes between 2.0 and 6.0 THz contribute about 68% (0.70) to the value of λ. This contribution is quite normal because the phonon DOS in this frequency region exhibits a dominance of As atoms with considerable contribution from Ru atoms. We have known that the As-like DOS around the Fermi level is the strongest while the Ru-like DOS around the Fermi level is considerable. The most interesting feature of the spectral function for $LaRu_4As_{12}$ is that the value of λ for $LaRu_4As_{12}$ increases almost linearly in the high-frequency region between 6.0 and 8.3 THz. Phonon modes in this frequency region make a contribution of about 21% (0.22) to the value of λ due to strong hybridization between As-related and Ru-related vibrations.

Finally, we analyze the spectral function contribution to the value of λ for $LaPt_4Ge_{12}$. The value of λ for $LaPt_4Ge_{12}$ scales up rapidly with increasing frequency up to 5.0 THz. However, its value rises like a small step function in the narrow frequency region between 5.0 and 5.7 THz. Finally, its value goes up linearly above 5.7 THz. In particular, different from $LaRu_4As_{12}$, phonon modes below 2.0 THz make a large contribution, around 40% (0.43), to the value of λ. This large contribution is not surprising because these phonon modes arise from Ge-La coupled oscillations. Thus, due to large contribution from Ge-related vibrations, the acoustic phonon branches in $LaPt_4Ge_{12}$ are more involved in the process of scattering of electrons as compared to the corresponding phonon branches in the remaining materials. The contribution of the frequency region between 2.0 and 5.0 THz to λ is around 44% (0.48). This large contribution is also acceptable because Ge-related vibrations are dominant in this frequency region. Now, we can state that these medium-frequency phonon modes are also involved in the process of scattering of electrons. Finally, phonon modes above 5.0 THz contribute about 16% (0.17) to the value of λ.

The parameters related to superconductivity in all the studied compounds are presented and compared with available experimental results in Table IV. The calculated values for λ are 0.74, 1.03, and 1.08 for $LaRu_4P_{12}$, $LaRu_4As_{12}$, and

TABLE IV. The superconducting state parameters for $LaRu_4P_{12}$, $LaPt_4Ge_{12}$, and $LaRu_4As_{12}$ and their comparison with available experimental results.

Superconductor	$N(E_F)$ (states/eV)	$\omega_{\ln}$ (K)	λ	T_C (K)
$LaRu_4P_{12}$	6.70	227	0.74	6.95
Experiment [38]	7.14		0.57	7.2
$LaPt_4Ge_{12}$	9.60	122	1.08	8.32
Experiment [49,51]				8.27
$LaRu_4As_{12}$	11.19	185	1.03	11.56
Experiment [37]			0.86	10.3
Experiment [46]				10.45

$LaPt_4Ge_{12}$, respectively. These results suggest that electron-phonon interaction in $LaRu_4P_{12}$ is of medium strength but the other two materials are characterized with the electron-phonon interaction of strong strength. Although the value of $N(E_F)$ is the largest for $LaRu_2As_{12}$, its λ is slightly smaller than that for $LaPt_4Ge_{12}$. This can be related to its larger ω_{ln} value of 185 K as compared to the corresponding value of 122 K for $LaPt_4Ge_{12}$ because the hardening of phonon frequencies tends to reduce the value of λ according to the McMillan-Hopfield expression. Our calculated values for T_c are 6.95, 11.56, and 8.32 K for $LaRu_4P_{12}$, $LaRu_4As_{12}$, and $LaPt_4Ge_{12}$, which are consistent with their experimental values of 7.2, 10.45, and 8.23 K [38,46,49].

IV. SUMMARY

This theoretical work has presented the structural, elastic, electronic, vibrational, and electron-phonon interaction properties of LaT_4X_{12} by using the generalized gradient approximation of the density functional theory and the plane-wave pseudopotential method. The calculated structural parameters for these lanthanum filled-skutterudite compounds accord very well with previous theoretical and experimental results while their calculated elastic constants confirm the mechanical stability of them. The calculated elastic constants for $LaPt_4Ge_{12}$ reveal that this material behaves in a ductile manner and is thus more readily machinable from the point of applications. Our electronic results for all the studied compounds indicate that the contribution of La to valence bands is very small due a charge transfer from it to the $[T_4X_{12}]$ polyanion. This indicates that superconductivity in these materials is intrinsic to the $[T_4X_{12}]$ polyanion while La electronically stabilizes their structure. Furthermore, a trademark feature of these filled-skutterudite compounds is the existence of a flat band very close to the Fermi level, which causes a peak in the density of states and thus gives rise to an enhancement of the superconducting properties in these materials. Phonon calculations indicate that these filled lanthanum skutterudites are dynamically stable in their body-centered-cubic structure. The phonon spectrum in $LaRu_4P_{12}$ is much wider in frequency range than its counterparts in the remaining materials due to its smaller lattice constant and smaller total masses as compared to the remaining materials.

An examination of the Eliashberg function for $LaRu_4P_{12}$ indicates that the optical phonon modes lying between 3.0 and 6.5 make the largest contribution to the value of λ due to the coupled motion of Ru and P atoms. In contrast, the value of λ for $LaRu_4As_{12}$ rises considerably with increasing phonon frequency in the whole frequency range. Thus, even high-frequency phonon modes of $LaRu_4As_{12}$ are significantly involved in the process of scattering of electrons. Different from $LaRu_4P_{12}$ and $LaRu_4As_{12}$, low-frequency phonon modes below 2.0 THz make a large contribution to the value of λ for $LaPt_4Ge_{12}$ because they are due to the coupled motion of Ge and La atoms. By integrating the Eliashberg spectral function, the average electron-phonon coupling parameter λ is obtained to be 0.74 for $LaRu_4P_{12}$, 1.03 for $LaRu_4As_{12}$, and 1.08 for $LaPt_4Ge_{12}$. These results reveal that all these lanthanum filled-skutterudite compounds are phonon-mediated superconductors but electron-phonon interaction in $LaRu_4As_{12}$ and $LaPt_4Ge_{12}$ is stronger than that in $LaRu_4P_{12}$. Using the Allen-Dynes modified McMillan equation with the screened Coulomb pseudopotential parameter $\mu^* = 0.13$, the superconducting temperature is obtained to be 6.95 K for $LaRu_4P_{12}$, 11.56 K for $LaRu_4As_{12}$, and 8.32 K for $LaPt_4Ge_{12}$. These values are in good accordance with their experimentally measured values of 7.2, 10.45, and 8.23 K.

ACKNOWLEDGMENT

Some of the calculations for this project were carried out using the computing facilities on the Intel Nehalem (i7) cluster (ceres) in the School of Physics, University of Exeter, United Kingdom.

[1] B. C. Sales, D. Mandrus, and R. K. Williams, Science **272**, 1325 (1996).
[2] V. Keppens, D. Mandrus, B. C. Sales, B. C. Chakoumakos, P. Dai, R. Coldea, M. B. Maple, D. A. Gajewski, E. J. Freeman, and S. Bennington, Nature (London) **395**, 876 (1998).
[3] G. S. Nolas, D. T. Morelli, and T. M. Tritt, Annu. Rev. Mater. Sci. **29**, 89 (1999).
[4] G. J. Snyder and E. S. Toberer, Nat. Matter. **7**, 105 (2008).
[5] N. R. Dilley, E. J. Freeman, E. D. Bauer, and M. B. Maple, Phys. Rev. B **58**, 6287 (1998).
[6] N. Takeda and M. Ishikawa, J. Phys.: Condens. Matter **13**, 5971 (2001).
[7] M. E. Danebrock, B. Christroph, H. Evers, and W. Jeitschko, J. Phys. Chem. Solids **57**, 381 (1996).
[8] C. Sekine, T. Uchiumi, I. Shirotani, K. Matsuhira, T. Sakakibara, T. Goto, and T. Yagi, Phys. Rev. B **62**, 11581 (2000).
[9] K. Hachitani, H. Fukazawa, Y. Kohori, I. Watanabe, C. Sekine, and I. Shirotani, Phys. Rev. B **73**, 052408 (2006).
[10] C. Sekine, T. Uchiumi, I. Shirotani, and T. Yagi, Phys. Rev. Lett. **79**, 3218 (1997).
[11] H. Sugawara, T. D. Matsuda, K. Abe, Y. Aoki, H. Sato, S. Nojiri, Y. Inada, R. Settai, and Y. Ōnuki, Phys. Rev. B **66**, 134411 (2002).
[12] S. H. Curnoe, K. Ueda, H. Harima, and K. Takegahara, J. Phys. Chem. Solids **63**, 1207 (2002).

[13] I. Shirotani, J. Hayashi, T. Adachi, C. Sekine, T. Kawakami, T. Nakanishi, H. Takahashi, J. Tang, A. Matsushita, and T. Matsumoto, Physica B **322**, 408 (2002).

[14] S. H. Curnoe, H. Harima, K. Takegahara, and K. Ueda, Phys. Rev. B **70**, 245112 (2004).

[15] H. Hidaka, I. Ando, H. Kotegawa, T. C. Kobayashi, H. Harima, M. Kobayashi, H. Sugawara, and H. Sato, Phys. Rev. B **71**, 073102 (2005).

[16] H. Suderow, K. Behnia, I. Guillamon, V. Crespo, S. Vieira, D. Kikuchi, Y. Aoki, H. Sugawara, and H. Sato, Phys. Rev. B **77**, 153101 (2008).

[17] F. Grandjean, A. Gerard, D. J. Braung, and W. Jeitschko, J. Phys. Chem. Solids **45**, 877 (1984).

[18] I. Shirotani, T. Uchiumi, C. Sekine, M. Hori, and S. Kimura, J. Solid State Chem. **142**, 146 (1999).

[19] C. H. Lee, H. Oyanagi, C. Sekine, I. Shirotani, and M. Ishii, Phys. Rev. B **60**, 13253 (1999).

[20] C. Sekine, N. Hoshi, K. Takeda, T. Yoshida, I. Shirotani, K. Matsuhira, M. Wakeshima, and Y. Hinatsu, J. Magn. Magn. Mater. **310**, 260 (2007).

[21] K. Nouneh, A. H. Reshak, S. Auluck, I. V. Kityk, R. Viennois, S. Benet, and S. Charar, J. Alloys Compd. **437**, 39 (2007).

[22] A. Shankar, D. P. Rai, Sandeep Chettri, R. Khenata, and R. K. Thapa, J. Solid State Chem. **240**, 126 (2016).

[23] A. Shankar, D. P. Rai, Sandeep, R. Khenata, R. K. Thapa, and P. K. Mandal, J. Alloys Compd. **672**, 98 (2016).

[24] E. D. Bauer, N. A. Frederick, P.-C. Ho, V. S. Zapf, and M. B. Maple, Phys. Rev. B **65**, 100506(R) (2002).

[25] H. Kotegawa, M. Yogi, Y. Imamura, Y. Kawasaki, G.-q. Zheng, Y. Kitaoka, S. Ohsaki, H. Sugawara, Y. Aoki, and H. Sato, Phys. Rev. Lett. **90**, 027001 (2003).

[26] R. Vollmer, A. Faißt, C. Pfleiderer, H. v. Löhneysen, E. D. Bauer, P.-C. Ho, V. Zapf, and M. B. Maple, Phys. Rev. Lett. **90**, 057001 (2003).

[27] K. Kuwahara, K. Iwasa, M. Kohgi, K. Kaneko, N. Metoki, S. Raymond, M.-A. Méasson, J. Flouquet, H. Sugawara, Y. Aoki, and H. Sato, Phys. Rev. Lett. **95**, 107003 (2005).

[28] H. Sugawara, M. Kobayashi, S. Osaki, S. R. Saha, T. Namiki, Y. Aoki, and H. Sato, Phys. Rev. B **72**, 014519 (2005).

[29] G. Seyfarth, J. P. Brison, M.-A. Méasson, J. Flouquet, K. Izawa, Y. Matsuda, H. Sugawara, and H. Sato, Phys. Rev. Lett. **95**, 107004 (2005).

[30] G. Seyfarth, J. P. Brison, M.-A. Méasson, D. Braithwaite, G. Lapertot, and J. Flouquet, Phys. Rev. Lett. **97**, 236403 (2006).

[31] C. R. Rotundu, P. Kumar, and B. Andraka, Phys. Rev. B **73**, 014515 (2006).

[32] T. R. Abu Alrub and S. H. Curnoe, Phys. Rev. B **76**, 054514 (2007).

[33] R. W. Hill, Shiyan Li, M. B. Maple, and Louis Taillefer, Phys. Rev. Lett. **101**, 237005 (2008).

[34] D. E. MacLaughlin, A. D. Hillier, J. M. Mackie, Lei Shu, Y. Aoki, D. Kikuchi, H. Sato, Y. Tunashima, and H. Sugawara, Phys. Rev. Lett. **105**, 019701 (2010).

[35] T. Keiber, F. Bridges, R. E. Baumbach, and M. B. Maple, Phys. Rev. B **86**, 174106 (2012).

[36] P.-C. Ho, D. E. MacLaughlin, Lei Shu, O. O. Bernal, Songrui Zhao, A. A. Dooraghi, T. Yanagisawa, M. B. Maple, and R. H. Fukuda, Phys. Rev. B **89**, 235111 (2014).

[37] I. Shirotani, T. Uchiumi, K. Ohno, C. Sekine, Y. Nakazawa, K. Kanoda, S. Todo, and T. Yagi, Phys. Rev. B **56**, 7866 (1997).

[38] T. Uchiumi, I. Shirotani, C. Sekine, S. Todo, T. Yagi, Y. Nakazawa, and Kazushi Kanoda, J. Phys. Chem. Solids **60**, 689 (1999).

[39] I. Shirotani, K. Ohno, C. Sekine, T. Yagi, T. Kawakami, T. Nakanishi, H. Takahashi, J. Tang, A. Matsushita, and T. Matsumoto, Physica B **281–282**, 1021 (2000).

[40] S. Tsuda, T. Yokoya, T. Kiss, T. Shimojina, S. Shin, T. Togais, S. Watanabe, C. Q. Zhang, C. T. Chen, H. Sugawara, H. Sato, and H. Harima, J. Phys. Soc. Jpn. **75**, 064711 (2006).

[41] M. Shimizu, H. Amanuka, K. Hachitani, H. Fukazawa, Yoh Kohori, T. Namiki, C. Sekine, and I. Shirptani, J. Phys. Soc. Jpn. **77**, 229 (2008).

[42] Y. Nakai, Y. Hayashi, K. Kitagawa, K. Ishida, H. Sugawara, D. Kikuchi, and H. Sato, J. Phys. Soc. Jpn. **77**, 333 (2008).

[43] T. Namiki, C. Senike, K. Matsuhira, M. Wakeshima, and I. Shirotani, J. Phys. Soc. Jpn. **77**, 336 (2008).

[44] K. Matsuhira, C. Sekine, M. Wakeshima, Y. Hinatsu, T. Namiki, K. Takeda, I. Shirotani, H. Sugawara, D. Kikuchi, and H. Sato, J. Phys. Soc. Jpn. **78**, 124601 (2009).

[45] J. Hayashi, K. Akahira, K. Matsui, H. Ando, Y. Sugiuchi, K. Takeda, C. Sekine, I. Shirotani, and T. Yagi, J. Phys.: Conf. Ser. **215**, 012142 (2010).

[46] L. Bochenek, R. Wawryk, Z. Henkie, and T. Cichorek, Phys. Rev. B **86**, 060511(R) (2012).

[47] X. Y. Tee, H. G. Luo, T. Xiang, D. Vandervelde, M. B. Salamon, H. Sugawara, H. Sato, C. Panagopoulos, and Elbert E. M. Chia, Phys. Rev. B **86**, 064518 (2012).

[48] E. Bauer, A. Grytsiv, Xing-Qiu Chen, N. Melnychenko-Koblyuk, G. Hilscher, H. Kaldarar, H. Michor, E. Royanian, G. Giester, M. Rotter, R. Podloucky, and P. Rogl, Phys. Rev. Lett. **99**, 217001 (2007).

[49] R. Gumeniuk, W. Schnelle, H. Rosner, M. Nicklas, A. Leithe-Jasper, and Yu. Grin, Phys. Rev. Lett. **100**, 017002 (2008).

[50] M. Toda, H. Sugawara, Ko-ichi Magishi, T. Saito, K. Koyama, Y. Aoki, and H. Sato, J. Phys. Soc. Jpn. **77**, 124702 (2008).

[51] R. Gumeniuk, H. Borrmann, A. Ormeci, H. Rosner, W. Schnelle, M. Nicklas, Y. Grin, and A. Leithe-Jasper, Z. Kristallogr. Cryst. Mater. **225**, 531 (2010).

[52] Y. Nakamura, H. Okazaki, R. Yoshida, T. Wakita, H. Takeya, K. Hirata, M. Hirai, Y. Muraoka, and T. Yokoya, Phys. Rev. B **86**, 014521 (2012).

[53] J. L. Zhang, G. M. Pang, L. Jiao, M. Nicklas, Y. Chen, Z. F. Weng, M. Smidman, W. Schnelle, A. Leithe-Jasper, A. Maisuradze, C. Baines, R. Khasanov, A. Amato, F. Steglich, R. Gumeniuk, and H. Q. Yuan, Phys. Rev. B **92**, 220503(R) (2015).

[54] H. Pfau, M. Nicklas, U. Stockert, R. Gumeniuk, W. Schnelle, A. Leithe-Jasper, Y. Grin, and F. Steglich, Phys. Rev. B **94**, 054523 (2016).

[55] F. Kanetake, H. Mukuda, Y. Kitaoka, Ko-ichi Magishi, H. Sugawara, K. M. Itoh, and E. E. Haller, J. Phys. Soc. Jpn. **79**, 063702 (2010).

[56] L. S. Sharath Chandra, M. K. Chattopadhyay, S. B. Roy, and Sudhir K. Pandey, Philos. Mag. **96**, 2161 (2016).

[57] H. Harima, Prog. Theor. Phys. Suppl. **138**, 117 (2000).

[58] K. Takegahara and H. Harima, J. Magn. Magn. Mater. **310**, 861 (2007).

[59] M. Chen, Ph.D. thesis, University of Vienna, Austria, 2012.

[60] S. Ram, V. Kanchana, and M. C. Valsakumar, J. Appl. Phys. **115**, 093903 (2014).

[61] J. P. Perdew, K. Burke, and M. Ernzerhof, Phys. Rev. Lett. **77**, 3865 (1996).
[62] C. Sekine, H. Saito, T. Uchiumi, A. Sakai, and I. Shirotani, Solid. State Commun. **106**, 441 (1998).
[63] C. Sekine, H. Saito, A. Sakai, and I. Shirotani, Solid. State Commun. **109**, 449 (1999).
[64] N. Ogita, T. Kondo, T. Hasegawa, Y. Takasu, M. Udagawa, N. Takeda, K. Ishikawa, H. Sugawara, D. Kikuchi, H. Sato, C. Sekine, and I. Shirotani, Physica B **383**, 128 (2006).
[65] M. M. Koza, D. A. Droja, N. T. Akeda, Z. Henkie, and T. C. Ichorek, J. Phys. Soc. Jpn. **82**, 114607 (2013).
[66] J. Bardeen, L. N. Cooper, and J. R. Schrieffer, Phys. Rev. **108**, 1175 (1957).
[67] P. Giannozzi, S. Baroni, N. Bonini, M. Calandra, R. Car, C. Cavazzoni, D. Ceresoli, G. L. Chiarotti, M. Cococcioni, I. Dabo, A. D. Corso, S. de Gironcoli, S. Fabris, G. Fratesi, R. Gebauer, U. Gerstmann, C. Gougoussis, A. Kokalj, M. Lazzeri, L. Martin-Samos, N. Marzari, F. Mauri, R. Mazzarello, S. Paolini, A. Pasquarello, L. Paulatto, C. Sbraccia, S. Scandolo, G. Sclauzero, A. P. Seitsonen, A. Smogunov, P. Umari, and R. M. Wentzcovitch, J. Phys.: Condens. Matter **21**, 395502 (2009).
[68] A. B. Migdal, Sov. Phys. JETP **34**, 996 (1958).
[69] G. M. Eliashberg, Zh. Eksp. Teor. Fiz. **38**, 966 (1960) [Sov. Phys. JETP **11**, 696 (1960)].
[70] C. Hartwigsen, S. Goedecker, and J. Hutter, Phys. Rev. B **58**, 3641 (1998).
[71] W. Kohn and L. J. Sham, Phys. Rev. **140**, A1133 (1965).
[72] H. J. Monkhorst and J. D. Pack, Phys. Rev. B **13**, 5188 (1976).
[73] F. D. Murnaghan, Proc. Natl. Acad. Sci. USA **50**, 697 (1944).
[74] M. J. Mehl, J. E. Osburn, D. A. Papaconstantopoulos, and B. M. Klein, Phys. Rev. B **41**, 10311 (1990).
[75] R. Hill, Proc. Phys. Soc. London A **65**, 349 (1952).
[76] W. Voigt, *Lehrbuch der Kristallphysik* (Taubner, Leipzig, 1928).
[77] A. Reuss, Z. Angew. Math. Mech. **9**, 49 (1929).
[78] O. L. Anderson, J. Phys. Chem. Solids **24**, 909 (1963).
[79] P. B. Allen and R. C. Dynes, Phys. Rev. B **12**, 905 (1975).
[80] M. Born and K. Huang, *Dynamical Theory of Crystal Lattices* (Clarendon, Oxford, U.K., 1956).
[81] F. Pugh, Philos. Mag. **45**, 823 (1954).